

Effect of Zn and Ni impurities on the quasiparticle renormalization in Bi-2212

V. B. Zabolotny,¹ S. V. Borisenko,¹ A. A. Kordyuk,^{1,2} J. Fink,¹ J. Geck,¹ A. Koitzsch,¹ M. Knupfer,¹ B. Büchner,¹ H. Berger,³ A. Erb,⁴ C. T. Lin,⁵ B. Keimer,⁵ and R. Follath⁶

¹*Institute for Solid State Research, IFW-Dresden, P.O.Box 270116, D-01171 Dresden, Germany*

²*Institute of Metal Physics of National Academy of Sciences of Ukraine, 03142 Kyiv, Ukraine*

³*Institute of Physics of Complex Matter, EPFL, CH-1015 Lausanne, Switzerland*

⁴*Walther-Meißner-Institut, Bayerische Akademie der Wissenschaften,*

Walther-Meißner Strasse 8, 85748 Garching, Germany

⁵*Max-Planck Institut für Festkörperforschung, D-70569 Stuttgart, Germany*

⁶*BESSY GmbH, Albert-Einstein-Strasse 15, 12489 Berlin, Germany*

The Cu substitution by Zn and Ni impurities and its influence on the mass renormalization effects in angle resolved photoelectron spectra (ARPES) of $\text{Bi}_2\text{Sr}_2\text{CaCu}_2\text{O}_{8-\delta}$ is addressed. We show that the nonmagnetic Zn atoms have much stronger effect both in nodal and antinodal parts of the Brillouin zone than magnetic Ni. The observed changes are consistent with the behaviour of the spin resonance mode as seen by inelastic neutron scattering in YBCO. This strongly suggests that the “peak-dip-hump” and the “kink” in ARPES on the one side and neutron resonance on the other are closely related features.

PACS numbers: 74.25.Jb, 74.72.Hs, 79.60.-i, 71.15.Mb

The unique sensitivity of the angle-resolved photoemission (ARPES) to the many-body effects in solids brings this technique to the forefront of the modern research in the field of high-temperature superconductivity (HTSC). The anomalies in the single-particle spectral function of a superconductor, detected and well characterized along the high symmetry directions, are commonly believed to be crucial for understanding HTSC. Along the nodal direction the renormalization effects are represented by the unusual dispersion, the so called “kink” [1, 2, 3]. In the vicinity of $(\pi, 0)$ point of the Brillouin zone (BZ), where the order parameter reaches its maximum, the renormalization is noticeably stronger and makes itself evident even in the lineshape of the single energy distribution curve (EDC)[4, 5, 6]. It is widely accepted that coupling to a collective mode [7, 8] naturally explains these anomalies. The origin of this mode remains a current controversy between two most frequently proposed candidates that are phonons and magnetic excitations.

Existing photoemission data suggest substantial dependence of the coupling between the electrons and the mode on momentum [2], hole doping [6, 9], and temperature [5, 10], which well fits the magnetic scenario. However, other similar ARPES experiments are interpreted in terms of phonons [11, 12]. In order to resolve this controversy one needs a way to vary separately either the phononic or magnetic spectrum. Variation in the phononic spectrum can be achieved by the use of different isotopes. Such an experiment for HTSC has recently been reported [13] but its “unusual” character (all major effects have been observed at high energies, 100-300 meV) leaves the problem of low-energy anomalies, which are relevant for the superconductivity, unsolved. In case of magnetic excitations, there is a possibility to change the magnetic spectrum via doping different types of impurities into the Cu-O plane. It is known from inelastic neutron scattering (INS) [14, 15] that substitution

of Zn and Ni leads to substantial changes in the magnetic spectrum.

In this paper we show that substitution of Zn and Ni essentially influences the renormalization anomalies in ARPES spectra both along the nodal and antinodal regions of the Brillouin zone. Moreover, the changes in ARPES spectra are in good correspondence to those observed in magnetic spectra by INS. This provides evidence that it is the magnetic excitations that are responsible for the unusual renormalization features in the quasiparticle excitation spectrum of cuprates.

The ARPES experiments were carried out at the U125/1-PGM beam line with an angle-multiplexing photoemission spectrometer (SCIENTA SES100) at BESSY. Overall energy resolution was set to 20 meV, and angular resolution was 0.2°, which yields a wave vector resolution 0.013 Å⁻¹ and 0.009 Å⁻¹ for 50 eV and 27 eV excitation energies, respectively. All data were acquired at $T = 30$ K in the superconducting state for three high quality samples: nearly optimally doped pure BSCCO ($T_C = 92$ K), Zn substituted BSCCO with nominal Zn concentration close to 1% ($T_C = 86$ K), and 2% Ni substituted BSCCO ($T_C = 87$ K).

We focused on two regions of the BZ, the nodal and the antinodal, which are schematically shown in a Fig.1 a by the two double-headed arrows. Here the solid red line stands for the bare dispersion of the antibonding band and the dashed blue one for the bonding band [16].

First we consider the antinodal region. In general case the EDC, the curve that represents distribution of photo-intensity as a function of energy at fixed momentum, taken at the $(\pi, 0)$ point (see panel a Fig 1) would consist of two peaks due to the bilayer split band [17]. It has been shown that the contribution from the bonding band can be completely removed by a proper choice of excitation energy [17](in this case $h\nu = 50$ eV). Nevertheless, at least for the underdoped samples [18], the line

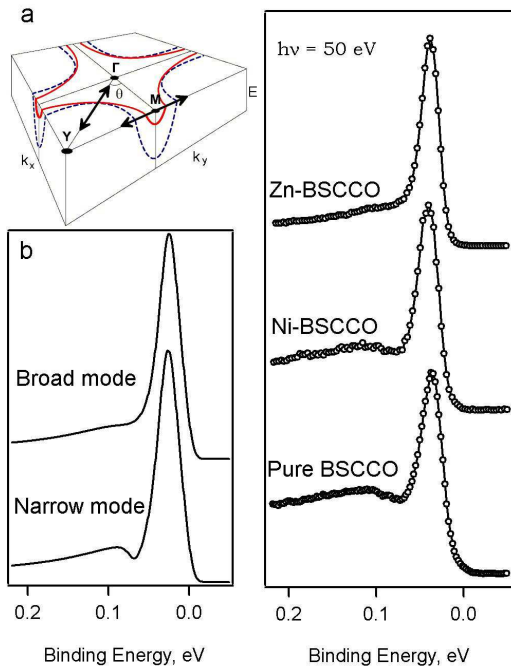


FIG. 1: (color). (a) Cut of a $k\omega$ -space at the Fermi level. The top of the cube contains two sheets of the Fermi surface, red solid line corresponds to the dispersion of the antibonding band, blue dashed one — to the bonding band. k_x and k_y axes are directed along the horizontal edges of the cube. (b) Model line shape of the $(\pi, 0)$ EDC, when coupled to a narrow (2 meV) and broad (20 meV) collective mode. (c) Experimental EDC taken at $(\pi, 0)$ point.

shape is not reduced to a single peak and has a dip at a higher binding energy. The appearance of the dip in a single band EDC is well explained in terms of coupling to a collective mode [7, 8]. Such an interaction with a sharp mode with energy Ω_{mode} leads to the increase of the scattering rate at binding energies higher than $\Omega_{mode} + \Delta$, where Δ is a superconducting gap, i.e. to a step like feature in the imaginary part of the self-energy and a logarithmic divergence in the real part of the self-energy giving rise to a dip in photoemission line shape. When the mode has a finite width the dip smears out as demonstrated in Fig. 1 b. Therefore, the dip can be a good indicative of the mode width and energy. Broadening of the mode described above well correspond to our experimental data presented in panel (c) of Fig. 1. Comparing these EDC's, measured at $(\pi, 0)$ point with 50 eV photon energy, we see a striking difference in the lineshapes caused by the impurity substitution: while for the pure sample the spectrum has a pronounced dip, for the Zn substituted sample the dip almost completely vanishes. For the Ni substituted sample the dip “strength” is intermediate. The dip vanishing with Zn doping is a robust effect that we observed for numerous samples and was one of the reasons to conduct this systematic study.

Another change in the spectra that one can notice is an

increase of the intensity of the low-energy peak relative to the spectral weight at higher binding energies upon Ni substitution and even stronger effect on Zn substitution. In a simple model where we explain the spectral weight at the $(\pi, 0)$ point by a strong coupling to a mode (e.g. the neutron resonance mode) such an intensity variation could be accounted for by a stronger coupling to the mode upon impurity substitution. A higher coupling to the mode would be related to a larger imaginary part of the self-energy and this would cause a stronger broadening and therefore a reduction of the intensity in the “hump” region. On the other hand such a broadening would also result in a flattening of the hump that we do not observe here. In addition, we do not see in the dispersion of the bonding band (not shown) any clear evidence for an increase of the mass enhancement with Zn doping. Thus, in order to account for all changes in the line shape one needs a model that also takes into consideration possible difference in elastic scattering contributions (e.g. due to different surface qualities) and different extrinsic backgrounds.

Now we turn to the nodal direction The nodal cuts (Fig. 2, a-c) were measured strictly along the BZ diagonal. The aforementioned position in k -space was guaranteed by the measured maps. In addition it was double

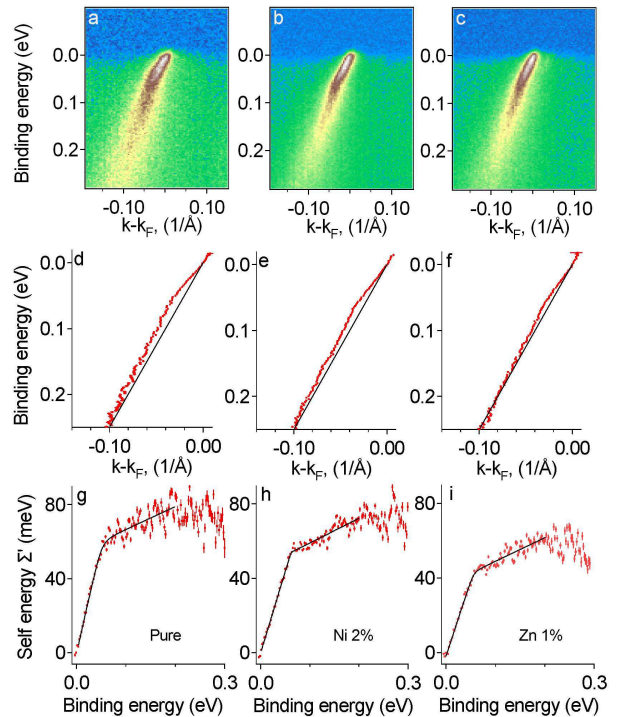


FIG. 2: (color). (a)-(c) Photo intensity distribution in the nodal cuts. (a) Pure BSCCO, (b) Ni substituted and (c) Zn substituted BSCCO. Middle row shows corresponding experimental dispersion. In the last row the real part of the self-energy obtained by subtractions of the bare band is displayed. The black solid lines are guides to eye, while the red symbols represent the data points.

checked using the steepest experimental dispersion as a criterion for the true nodal cut. Since the nodal region is also complicated by bilayer splitting [19], the matter of excitation energy remains important here too. The nodal spectra were measured with $h\nu = 27$ eV, when again only one of the bilayer split bands is visible [19]. In the second row of Fig. 2 we show the experimental dispersion obtained from the maxima position of the Lorentzians that provide the best fit to the momentum dispersion curves (MDC). The straightforward way to estimate a degree of the renormalization effects is to draw one and the same “guide” line from the Fermi level to some fixed point on the experimental dispersion curve and treat the area between the dispersion curve and the guide line as an effective measure of renormalization. It is easy to see that renormalization in case of the Zn substituted sample is decreased in comparison to the pure sample. Subtracting a bare particle band from the experimental dispersion the real part of the self-energy can be obtained. Here, as follows from a self-consistent Kramers-Krönig procedure [20], for the bare band dispersion we used a parabolic band with its bottom lying 0.8 eV below the Fermi level (FL). Defining a coupling constant as derivative of the real part of the self-energy at the FL we find that $\lambda_{pure} \approx 1.06$, $\lambda_{Ni} \approx 0.88$, and for the Zn doped sample it has the lowest value $\lambda_{Zn} \approx 0.76$. We note that, although the obtained absolute values for λ depend on the parameters of the bare band dispersion, their ratio remains almost insensitive to the position of the bottom of the bare band, provided that the bare band is the same for all three samples. Therefore more accurate would be to say that the coupling constant for the nodal direction is reduced by approximately 15% for the 2% Ni doped sample and by 30% for 1% Zn doped sample as compared to pure one.

A link between the modifications in our spectra and changes in the spectrum of magnetic excitations with impurity substitution was based on the implication that we have equal charge doping of the samples. It is known that the renormalization features are weakening with overdoping both in nodal and antinodal directions [6, 9]. Therefore different hole doping might be a possible explanation. In order to evaluate the hole doping level we measured the maps in k space for all samples, which, in addition, allowed us to know precisely our position in the reciprocal space when measuring nodal and antinodal spectra. In a false colour scale (Fig.3) we show experimental data, which are the cuts of $k\omega$ -space made 20 meV below the Fermi level for the three samples under consideration (a - c). For comparison, in the panel d we give the identical cut for overdoped sample with the hole doping δ within 0.19 – 0.20. Grey scale images below the experimental data represent tight-binding fits to the antibonding sheet of the Fermi surface (FS) [21]. We focus attention on the “lens” (Fig. 3 d) formed by the shadow and the 1st order diffraction replica. Even from its size, which is determined by the size of the FS, it is clear that the first three samples have very close

hole doping, and that the doping of the fourth sample is notably higher. To be quantitative, the area of antibonding sheets of the FS cuts can be used as a good relative doping measure. Evaluation gives the following result: $(S_a - 1/2) : (S_b - 1/2) : (S_c - 1/2) : (S_d - 1/2) \approx 1.00 : 1.01 : 0.98 : 1.14$, where S_i denotes the ratio of the area confined by one “barrel” to the area of the whole BZ. The values for S_i were obtained from the tight-binding fit of experimental map for each panel (a-d). However, a charge doping induced suppression of the renormalization features would require a deviation of the hole concentration of about 30 % [6]. So we see that the difference in charge doping for our sample is negligible to account for substantial change in the line shape (Fig. 1 c) at the antinode, as well as for the different renormalization constants (Fig. 2) for the nodal spectra.

We find that our experimental observations of the dip smearing in the antinodal EDC are in good agreement with the results of inelastic neutron scattering (INS) experiments. The comparison with INS is most pertinent here, since it gives a detailed insight into the changes in the spectrum of magnetic excitations produced by the impurities and allows to make a comparison with those that we see in ARPES spectra. The direct observation of the magnetic resonance mode by INS in YBCO demonstrates its strong sensitivity to impurities incorporated into Cu-O planes. When for pure sample the mode is sharply peaked at ~ 40 meV with a FWHM being resolution limited [22], for 1% Zn substituted YBCO the mode attains finite width of about 10 meV[14]. Grad-

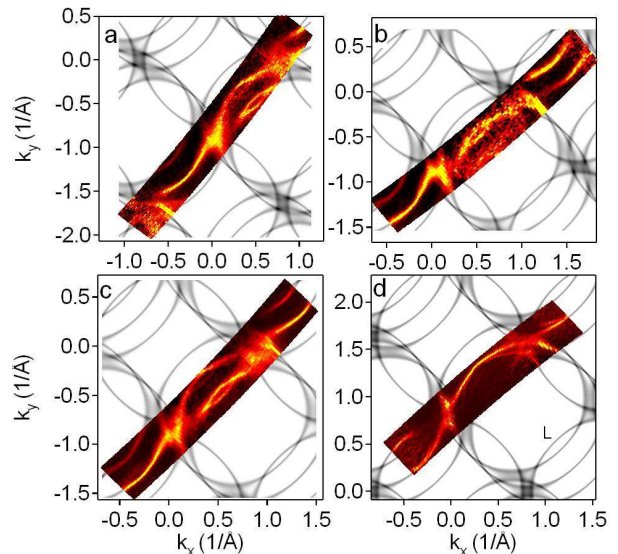


FIG. 3: (color). Cuts of $k\omega$ -space made 20 meV below the Fermi level and tight binding fits. (a) Ni substituted sample. (b) Zn substituted sample. (c) Pure BSCCO close to optimal doping. (d) Overdoped BSCCO, $\delta \approx 0.20$; letter L denotes “lens” formed by the shadow band and the 1st order diffraction replica.

ual broadening of the resonance and decrease of its peak intensity is traced in details in Ref. 15. From Ref. 14 it follows that introduction 3% of Ni result in approximately the same intensity of the resonance at its peak as in the case of 1% Zn doping, supporting the idea that nonmagnetic Zn has stronger influence on spin dynamics than Ni, which is the same that we see in ARPES spectra.

Raman scattering experiments on optimally doped YBCO [29] show that the A_{1g} electronic collective mode, that follows the acoustic part of magnetic resonance, gradually broadens with increase of Zn concentration. For 2% Zn substituted YBCO the A_{1g} mode almost disappears, while this is not the case for 3% Ni substituted YBCO where the mode loses only about half of its intensity [30]. It is also worth mentioning that Raman scattering experiments on Zn and Ni substituted YBCO crystals show no apparent changes in the structure of phonon anomalies [28, 31] at room temperature suggesting that the lattice dynamics remains unchanged. Similar results, except for the peak at 340 cm^{-1} , are obtained in Ref. 32 for superconducting state. This peak shows small decrease of its intensity and insignificant, as compared to magnetic resonance mode, broadening from 1.6 to 1.9 meV. It is clear that such a broadening cannot account for the vanishing of the dip in the $(\pi, 0)$ spectra. Therefore we conclude that the smearing of the dip in the APES antinodal spectra with impurities doping is a straightforward consequence of the magnetic resonance mode broadening, and possibly decrease of its integral intensity.

For the nodal direction the situation is more complicated. According to [23] the renormalization effects in nodal spectra are mainly caused by scattering of the electrons between nodes and Van Hove singularity in the density of states at $(\pi, 0)$ point by the resonance mode centered at antiferromagnetic vector $Q(\pi, \pi)$. This serves as a good explanation for the fact that the renormal-

ization effects are much weaker in the node than those in the vicinity of $(\pi, 0)$ point. But it also means, that the renormalization has to increase with the resonance mode broadening in momentum space when impurities are doped into Cu-O plaquette [14]. On the contrary, our observations show that the dimensionless coupling constant λ , decreases suggesting that the scattering by the antiferromagnetic vector $Q(\pi, \pi)$ does not have the dominant contribution in the nodal spectra renormalization effects [25]. The new resonance feature in magnetic excitation spectrum [26, 27] peaked at energy close to 54 meV and incommensurate vector $Q_{IC}^*(0.8\pi, 0.8\pi)$ provides scattering between the nodes, and therefore, should have a strong influence on the nodal spectra renormalization effects. However its evolution with impurity doping needs to be clarified, in order to check its pertinence for the problem in hand.

In conclusion, we have shown that the substitution of Cu atoms in Cu-O plane changes renormalization features in ARPES spectra both in nodal and antinodal parts of the Brillouin zone. The smearing of the dip in the antinodal EDC can be well explained by coupling of electrons to magnetic resonance mode. The effect of Zn and Ni substitution on the antinodal ARPES spectra is in good agreement with the influence of these impurities on magnetic resonance mode seen by INS experiments. These in addition to the previous ARPES studies of temperature and doping dependence [2, 6, 9, 19] of PDH structure, mass renormalization near antinodal region and a kink in a nodal part of Brillouin zone, provides another strong evidence that the mode, coupling to which, causes observed renormalization effects has rather magnetic than phononic origin.

The project is part of the Forschergruppe FOR538 and is supported by the DFG under Grants No. KN393/4 and No. 436UKR17/10/04. We acknowledge stimulating discussions with I. Eremin, and technical support by R. Hübel, S. Leger.

-
- [1] T. Valla *et al.*, *Science* **285**, 2110 (1999).
 - [2] P.V. Bogdanov *et al.*, *Phys. Rev. Lett.* **85**, 2581 (2000).
 - [3] A. Kaminski *et al.*, *Phys. Rev. Lett.* **86**, 1070 (2001).
 - [4] M.R. Norman *et al.*, *Phys. Rev. Lett.* **79**, 3506 (1997).
 - [5] A. D. Gromko *et al.*, *Phys. Rev. B.* **68**, 174520 (2003).
 - [6] T. K. Kim *et al.*, *Phys. Rev. Lett.* **91**, 167002 (2003).
 - [7] S. Engelsberg and J. R. Schrieffer, *Phys. Rev.* **131**, 993 (1963).
 - [8] A. W. Sandvik *et al.*, *Phys. Rev. B.* **69**, 094523 (2004).
 - [9] P. D. Johnson *et al.*, *Phys. Rev. Lett.* **87**, 177007 (2001).
 - [10] A. A. Kordyuk *et al.*, *Phys. Rev. Lett.* **92**, 257006 (2004).
 - [11] T. Cuk *et al.*, *Phys. Rev. Lett.* **93**, 117003 (2004).
 - [12] T. P. Devereaux *et al.*, *Phys. Rev. Lett.* **93**, 117004 (2004).
 - [13] A. Lanzara *et al.*, *Nature* **430**, 187 (2004).
 - [14] Y. Sidis *et al.*, *Phys. Rev. Lett.* **84**, 5900 (2000).
 - [15] Y. Sidis *et al.*, *cond-mat/0006265*.
 - [16] A. A. Kordyuk *et al.*, *Phys. Rev. B.* **67**, 064504 (2003).
 - [17] A. A. Kordyuk *et al.*, *Phys. Rev. Lett.* **89**, 077003 (2002).
 - [18] S. V. Borisenko *et al.*, *Phys. Rev. Lett.* **90**, 207001 (2003).
 - [19] A. A. Kordyuk *et al.*, *Phys. Rev. B.* **70**, 214525 (2004).
 - [20] A. A. Kordyuk *et al.*, *Phys. Rev. B.* **71**, 214513 (2005).
 - [21] O.K. Andersen *et al.*, *Phys. Chem. Solids* **56**, 1573 (1995).
 - [22] H. F. Fong *et al.*, *Phys. Rev. Lett.* **75**, 316 (1995).
 - [23] M. Eschrig *et al.*, *Phys. Rev. B.* **67**, 144503 (2003).
 - [24] H. F. Fong *et al.*, *Nature* **398**, 588 (1999).
 - [25] A. V. Chubukov *et al.*, *Phys. Rev. B.* **70**, 174505 (2004).
 - [26] S. Pailhes *et al.*, *Phys. Rev. Lett.* **93**, 167001 (2004).
 - [27] I. Eremin *et al.*, *Phys. Rev. Lett.* **94**, 147001 (2005).
 - [28] N. Watanabe *et al.*, *Phys. Rev. B.* **57**, 632 (1998).
 - [29] M. Le. Tacon *et al.*, *cond-mat/0504287*.
 - [30] Y. Gallais *et al.*, *Phys. Rev. Lett.* **88**, 177401 (2002).
 - [31] M. Käll *et al.*, *Phys. Rev. B.* **53**, 3566 (1996).
 - [32] M. Limonov *et al.*, *Phys. Rev. B.* **65**, 024515 (2001).